Spontaneous knotting of an agitated string

Dorian M. Raymer* and Douglas E. Smith*

Department of Physics, University of California at San Diego, 9500 Gilman Drive, Mail Code 0379, La Jolla, CA 92093

Edited by Leo P. Kadanoff, University of Chicago, Chicago, IL, and approved July 30, 2007 (received for review December 21, 2006)

It is well known that a jostled string tends to become knotted; yet the factors governing the "spontaneous" formation of various knots are unclear. We performed experiments in which a string was tumbled inside a box and found that complex knots often form within seconds. We used mathematical knot theory to analyze the knots. Above a critical string length, the probability *P* of knotting at first increased sharply with length but then saturated below 100%. This behavior differs from that of mathematical self-avoiding random walks, where *P* has been proven to approach 100%. Finite agitation time and jamming of the string due to its stiffness result in lower probability, but *P* approaches 100% with long, flexible strings. We analyzed the knots by calculating their Jones polynomials via computer analysis of digital photos of the string. Remarkably, almost all were identified as prime knots: 120 different types, having minimum crossing numbers up to 11, were observed in 3,415 trials. All prime knots with up to seven crossings were observed. The relative probability of forming a knot decreased exponentially with minimum crossing number and Möbius energy, mathematical measures of knot complexity. Based on the observation that long, stiff strings tend to form a coiled structure when confined, we propose a simple model to describe the knot formation based on random "braid moves" of the string end. Our model can qualitatively account for the observed distribution of knots and dependence on agitation time and string length.

Jones polynomial | knot energy | knot theory | random walk | statistical physics

Knots have been a subject of scientific study since as early as 1867, when Lord Kelvin proposed that atoms might be described as knots of swirling vortices (1). Although this theory fell into disfavor, it stimulated interest in the subject, and knots currently play a role in many scientific fields, including polymer physics, statistical mechanics, quantum field theory, and DNA biochemistry (2, 3). Knotting and unknotting of DNA molecules occurs in living cells and viruses and has been extensively studied by molecular biologists (4–6). In physics, spontaneous knotting and unknotting of vibrated ball-chains have recently been studied (7–9). In mathematics, knot theory has been an active field of research for more than a century (3).

Formation of knots in mathematical self-avoiding random walks has been extensively studied (10–16). In the 1960s, Frisch and Wasserman (10) and Delbruck (11) conjectured that the probability of finding a knot would approach 100% with an increasing walk length. In 1988, Sumners and Whittington (15) proved this conjecture rigorously by showing that exponentially few arcs would remain unknotted as the length tends to infinity. Numerical studies of finite-length random walks find that the probability of knotting and the average complexity of knots increase sharply with the number of steps (16).

Here, we describe a simple physical experiment on knot formation. A string was placed in a cubic box and the box was rotated at constant angular velocity about a principle axis perpendicular to gravity, causing the string to tumble. We investigated the probability of knotting, the type of knots formed, and the dependence on string length. Before tumbling, the string was held vertically above the center of the box and dropped in, creating a quasirandom initial conformation. After tumbling, the box was opened and the ends of the string were lifted directly upward and joined to form a closed loop. A digital photo was taken whenever a complex knot was formed. The experiment was repeated hundreds of times with each string length to collect statistics.

Results

Most of the measurements were carried out with a string having a diameter of 3.2 mm, a density of 0.04 g/cm, and a flexural rigidity of 3.1×10^4 dynes·cm^2, tumbling in a $0.30 \times 0.30 \times 0.30$-m box rotated at one revolution per second for 10 sec (see *Materials and Methods*). Photos of the string taken before and after tumbling are shown in Fig. 1, and movies of the tumbling are provided as supporting information (SI) Movies 1–5. The measured dependence of knotting probability *P* on string length *L* is shown in Fig. 2. No knots were obtained for $L < 0.46$ m, where SI Movie 1 shows that the confinement and tumbling did not induce sufficient bending to allow knot formation. As *L* was increased from 0.46 to 1.5 m, *P* increased sharply. However, as *L* was increased from 1.5 to 6 m, *P* saturated at ≈50%. The photos and movies show that when the string is confined in the box, the finite stiffness of the string results in its tending to form a coil (not perfectly, but to some degree) with a radius similar to the box width. During and after tumbling, this coiled structure is preserved, often with some compression of its radius perpendicular to the rotation axis (Fig. 1 and SI Movie 2).

A series of additional experiments were done to investigate the effect of changing the experimental parameters, as summarized in Table 1. Tripling the agitation time caused a substantial increase in *P*, indicating that the knotting is kinetically limited. Decreasing the rotation rate by 3-fold while keeping the same number of rotations caused little change in *P*. SI Movie 3 shows that effective agitation still occurs because the string is periodically carried upward along the box wall. A 3-fold increase in the rotation rate, on the other hand, caused a sharp decrease in *P*. SI Movie 4 shows that in this case, the string tends to be flung against the walls of the box by centrifugal force, resulting in less tumbling motion.

Doubling the box width increased *P* slightly, but decreasing it by 33% caused *P* to drop sharply. SI Movie 5 shows that the tumbling motion was reduced because the finite stiffness of the coiled string tends to wedge it more firmly against the walls of the box. We also did measurements with a stiffer string (see *Materials and Methods*) in the 0.15-m box and observed a substantial drop in *P*. Observations again revealed that the tumbling motion was reduced due to wedging of the string against the walls of the box. Conversely, measurements with a more flexible string found a substantial increase in *P*. With the longest length studied of this string (4.6 m), *P* reached 85%,

Author contributions: D.M.R. and D.E.S. designed research, performed research, analyzed data, and wrote the paper.

The authors declare no conflict of interest.

This article is a PNAS Direct Submission.

*To whom correspondence may be addressed. E-mail: draymer@physics.ucsd.edu or des@physics.ucsd.edu.

This article contains supporting information online at www.pnas.org/cgi/content/full/0611320104/DC1.

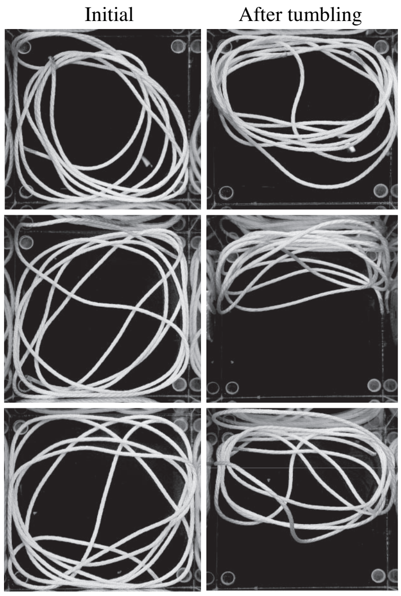

Fig. 1. Three examples of photos of the conformation of the string in the box before and after tumbling.

suggesting that P tends to 100% in the limit of long agitation time, long length, and high flexibility.

Topological Analysis and Knot Classification

A string can be knotted in many possible ways, and a primary concern of knot theory is to formally distinguish and classify all possible knots. A measure of knot complexity is the number of minimum crossings that must occur when a knot is viewed as a two-dimensional projection (3). In the 1920s, J. Alexander (17) developed a way to classify most knots with up to nine crossings by showing that each knot could be associated with a specific polynomial that constituted a topological invariant. In 1985, V. Jones (18) discovered a new family of polynomials that constitute even stronger topological invariants.

A major effort of our study was to classify the observed knots by using the concept of polynomial invariants from knot theory. When a random knot formed, it was often in a nonsimple configuration, making identification virtually impossible. We therefore developed a computer algorithm for finding a knot's Jones polynomial based on the skein theory approach introduced by L. Kauffmann (3, 19).

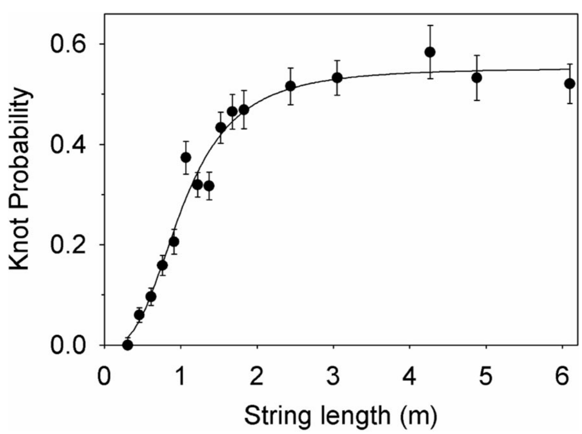

Fig. 2. Measured probability of forming a knot versus string length. The line is a least-squares fit to a simple sigmoidal function $N = N_0/(1 + (L/L_0)^b)$, with $N_0 = 0.55$, $L_0 = 3.4$, and $b = -2.9$.

This method involves enumerating all possible states of a diagram in which each crossing is "smoothed," meaning cut out and reconnected in one of two possible ways: $a = \asymp$ or $b =)($, resulting in $|S|$ closed loops. All crossings were identified, as illustrated in Fig. 3, each being either "over" or "under" and having a writhe (3) (or "handedness") of $+1$ or -1. This information was input into a computer program that we developed. The Kauffman bracket polynomial, in the variable t, was then calculated as

$$-t^{-3w}\sum_{S} t^{(N_a-N_b)}(-t^{2}-t^{-2})^{|S|-1}, \qquad [1]$$

where the sum is over all possible states S, N_a, and N_b are the numbers of each type of smoothing in a particular state, and w is the total writhe (3). The Jones polynomial is then obtained by the substitution $t \to t^{-1/4}$ and compared with polynomials in the enumerated *Table of Knot Invariants*.†

Strikingly, we were able to identify ≈96% of all knots formed (1,007 of 1,127)‡ as known prime knots having minimum crossing numbers ranging from 3 to 11. The prevalence of prime knots is rather surprising, because they are not the only possible type of knot. Computer simulations of random walks find an increasing fraction of nonprime "composite knots" with increasing length (14, 20). Here, only 120 of the knots were unclassifiable in 3,415 trials. Anecdotally, many of those were composite knots, such as pairs of 3_1 trefoils.

As shown in Fig. 4 *A* and *B*, the number of different types of knots observed (per number of trials) and the mean minimum crossing number $c(K)$ increased sharply with increasing string length for $L = 0.46$ to 1.5 m. However, for $L > 1.5$ m, both quantities saturated, along with the total knot probability. Knots with $c(K) = 3$ to 11 were observed and the mean $c(K)$ increased from ≈3 to 6. As shown in Fig. 4*C*, all possible prime knots with $c(K) = 3$, 4, 5, 6, and 7 were observed. Above $c(K) = 7$, the fraction of possible knots observed dropped dramatically because the number of possible knots grows faster than exponentially, rapidly exceeding the number of experimental trials.

Discussion

Although our experiments involve only mechanical motion of a one-dimensional object and occupation of a finite number of well defined topological states, the complexity introduced by knot formation raises a profound question: Can any theoretical framework, beside impractical brute-force calculation under Newton's laws, predict the formation of knots in our experiment?

Many computational studies have examined knotting of random walks. Although the conformations of our confined string are not just random walks (being more ordered), some similarities were observed. Specifically, computational studies find that the probability $1 - P$ of not forming a knot decreases exponentially with random walk length (13, 14). In our experiments with the medium-stiffness string, we find the same trend for lengths ranging from $L = 0.46$ to 1.5 m, but P approached a value of <1 as the length was increased further. As mentioned above, we attribute this to the finite agitation time.

In numerical studies of confined random walks (13, 20), P was found to increase with increasing confinement, and this effect has been proposed to explain the high probability of knotting of

†Livingston, C., Cha, J. C., *Table of Knot Invariants* (Indiana University; www.indiana.edu/~knotinfo). Accessed December 2006.

‡In a small fraction of cases, the Jones polynomial alone did not determine the knot. In 6 cases the knot was distinguished by visual inspection, in 19 cases it was distinguished by calculating the Alexander polynomial, and in 7 cases it was distinguished by calculating the HOMFLY polynomial (3).

Table 1. Dependence of knot probability on physical parameters

Condition	Box width 0.1 m	Box width 0.15 m	Box width 0.3 m
3-m length of #4 string, tumbled at one revolution per second for 10 sec	26%	50%	55%
Slower tumbling (0.33 revolutions per second)	29%	52%	57%
Faster tumbling (three revolutions per second)	8%	17%	20%
Longer tumbling time (30 sec)	30%	74%	63%
More flexible string, 3 m	—	65%	—
More flexible string, 4.6 m	—	85%	—
Stiffer string, 3 m	—	20%	—

The physical properties of the strings are given in *Materials and Methods*. The percentages were determined from 200 trials.

DNA confined in certain viruses (6). However, this trend is in contrast to that observed in our experiment. Our movies reveal that in our case, increasing confinement of a stiff string in a box causes increased wedging of the string against the walls of the box, which reduces the tumbling motion that facilitates knotting. Interestingly, a similar effect has also been proposed to restrict the probability of knotting of the umbilical cord of fetuses due to confinement in the amniotic sac (21).

Calculations on numerical random walks also find that the probability of occurrence of any particular knot decreases exponentially with its complexity, as measured by the minimum crossing number (16). We find that such behavior holds quite strikingly in our experiment as well (Fig. 5*A*). This finding

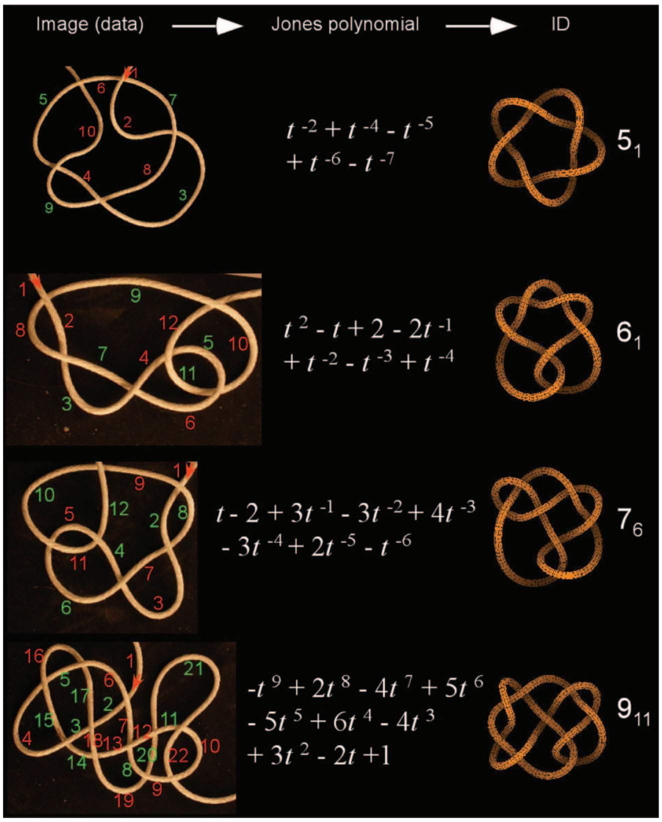

Fig. 3. Determinations of the knot identities by using polynomial invariants from knot theory. Digital photos were taken of each knot (*Left*) and analyzed by a computer program. The colored numbers mark the segments between each crossing. Green marks an under-crossing and red marks an over-crossing. This information is sufficient to calculate the Jones polynomial, as described in the text, allowing each knot to be uniquely identified. The simplified drawings (*Right*) were made by using KnotPlot [R. Scharein (December 2006), www.knotplot.com].

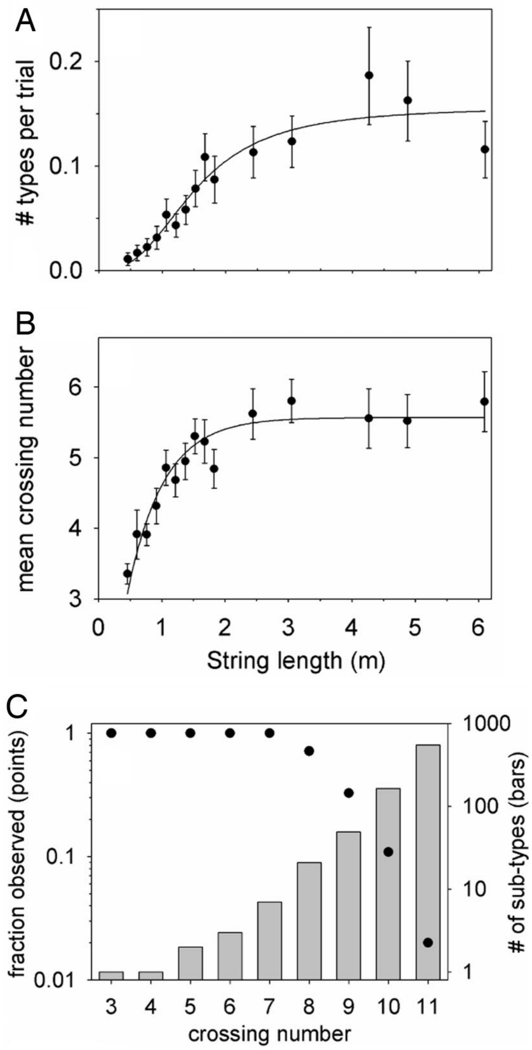

Fig. 4. Properties of the distribution of observed knot types. (*A*) Number of unique knots observed (per trial) vs. string length. The line is a fit to a simple sigmoidal function $N = N_0/(1 + (L/L_0)^b)$, with $N_0 = 0.16$, $L_0 = 5$ ft, and $b = -2.6$. (*B*) Mean minimum crossing number vs. string length. The line is a fit to a simple exponential function $P = P_0(1 - \exp(-bL))$, with $P_0 = 5.6$ and $b = 0.54$. (*C*) Fraction of total possible types observed vs. minimum crossing number (points), compared with the total number of types possible (bars).

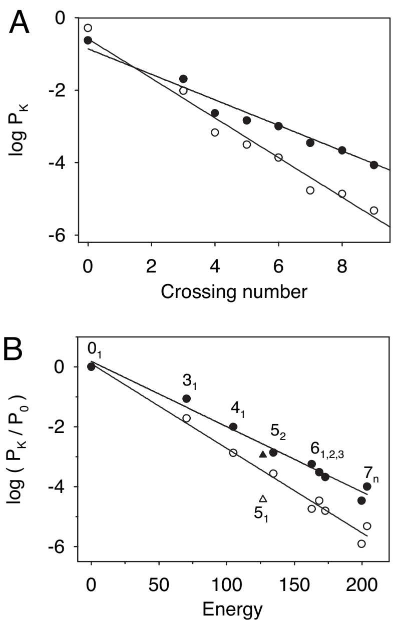

Fig. 5. Dependence of the probability of knotting on measures of knot complexity. (*A*) Natural log of P_K plotted versus theoretically calculated knot energy (25). (*B*) Natural log of the probability P_K of forming a certain knot plotted vs. minimum crossing number $c(K)$. Each value was normalized by the probability P_0 of forming the unknot. The filled circles are results with string lengths $L > 1.5$ m and the open circles are with $L <= 1.5$ m. The point styles are as in *A* except that the results with the 5_1 knot, which notably did not follow the overall trend, were plotted as triangles.

suggests that, although our string conformations are not random walks, random motions do play an important role.

Another measure of knot complexity is "knot energy." To investigate whether optimal spatial forms exist for knots, mathematicians have associated energy functions with knotted curves and sought minimizers (22–24). A class of functions studied in detail was inverse-power potentials, mimicking loops with uniform charge density. A regularized potential $\approx 1/r^2$ was found to be advantageous as the energy could be made scale-invariant and invariant under Möbius transformations. Freedman, He, and Wang (24) proved the existence of minimizers for such functions and set certain upper bounds on possible knot energies. Kusner and Sullivan (25) used a gradient descent algorithm to numerically calculate minimum energy states for many different knots and showed that they could distinguish different knots having the same minimum crossing number. Although our string shows no significant static charge (see *Materials and Methods*), its flexural rigidity would penalize complex knot formation in a qualitatively similar manner as the Möbius knot energy (23). In fact, we observe a strong correlation (an approximately exponential decrease) of the probability P_K of forming a certain knot with the minimum energies calculated in ref. 25 (Fig. 5*B*), although the 5_1 knot deviated notably from the trend.

Comparison with Previous Studies. Several previous studies have investigated knots in agitated ball-chains. Ben-Naim *et al.* (8) tied simple 3_1 knots in the chains and studied their unknotting on a vibrating plate. They found that the knot survival probability followed a universal scaling function independent of the chain length, and that the dynamics could be modeled by three random walks interacting via excluded volume in one spatial dimension.

Belmonte *et al.* (7) observed spontaneous knotting and unknotting of a driven hanging ball-chain. Various knots were formed, but only 3_1 and 4_1 knots were specifically identified. It was found that although 4_1 is more complex, it occurred more frequently than 3_1. Additional studies showed that the 3_1 knot (and other "torus knots"; e.g., 5_1 7_1, 9_1, 11_1) slips more easily off the bottom of the hanging chain (26). These experiments indicate that unknotting can have a strong influence on the probability of obtaining a certain knot after a fixed agitation time and may help to explain our observation of a lower probability for the 5_1 knot relative to the trend in Fig. 5*B* (although we note that 3_1 occurred with higher probability than 4_1 in our experiment).

Hickford *et al.* (9) recently examined the knotting and unknotting dynamics of a ball-chain on a vibrating plate. The chain was short enough that almost all of the knots were simple 3_1 knots and the tying and untying events could be detected by video image analysis. They found that the knotting rate was independent of chain length but that the unknotting rate increased rapidly with length. It was shown that the probability P of finding a knot after a certain time depended on the balance between tying and untying kinetics. Although our experimental geometry is different, our measured dependence of P on length (Fig. 2) is quite similar to that observed by Hickford *et al.*, suggesting that a similar mechanism may apply. In our study, however, the string is much longer, much more complex knots are formed, and we focus on characterizing the relative probabilities of formation of different knots.

Simplified Model for Knot Formation. Because the segments of a solid string cannot pass through each other, the principles of topology dictate that knots can only nucleate at the ends of the string. Roughly speaking, the string end must trace a path that corresponds to a certain knot topology in order for that knot to form. This process has been directly visualized for simple 3_1 knots in the studies of vibrated ball-chains (9). In principle, knots may form independently at both ends of the string, but principles of knot theory dictate that this would result in the formation of "nonprime" knots (3). For example, if a separate 3_1 knot is formed at each end of a string, they can be slid together at the center of the string but cannot merge to form a single prime knot. That the majority of the observed knots were prime suggests that knotting primarily occurs at one end of the string in our experiment. Therefore, in developing our model, we restricted our attention to the dynamics at one end and ignored the other end.

The photos and movies of our tumbled string show that string stiffness and confinement in the box promote a conformation consisting (at least partly) of concentric coils having a diameter on the order of the box size. Based on this observation, we propose a minimal, simplified model for knot formation, as illustrated schematically in Fig. 6. We assume that multiple parallel strands lie in the vicinity of the string end and that knots form when the end segment weaves under and over adjacent segments. Interestingly, our model corresponds closely to the mathematical representation of knots in a "braid diagram," and the weaving corresponds to "braid moves," which provides additional insights (3). The relationship between a braid diagram and a knot is established by the assumed connectivity of the group of line segments, as indicated by the dashed lines in the figure. One may ignore the local motions of these sections of the string because they cannot change the topology. In our simple model, we assume that the end segment makes random weaves, with a 50% chance of moving up vs. down and a 50% chance of moving under vs. over an adjacent segment. This model allows for both knotting and unknotting to occur.

Although this is a minimal, simplified model, we find that it can account for a number of the experimental results. First, according to a basic theorem of knot theory (27), all possible prime knots may be formed via such braid moves, consistent with our observation that all possible knots (at least up to seven crossings) are formed in our experiment. Second, the model can

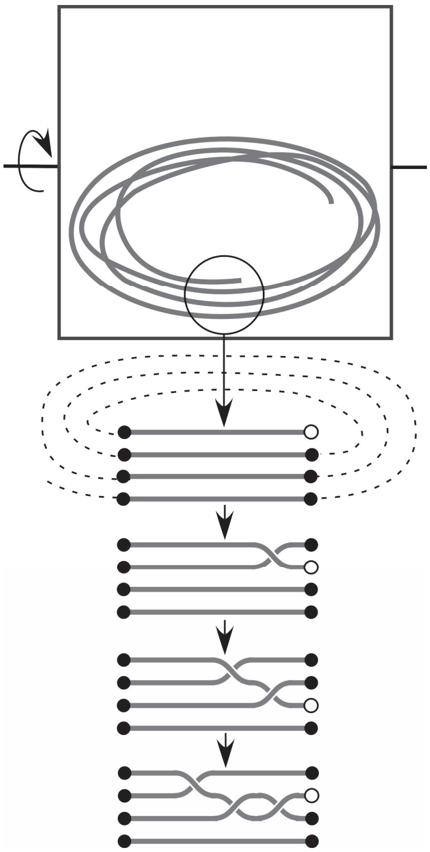

Fig. 6. Schematic illustration of the simplified model for knot formation. Because of its stiffness, the string tends to coil in the box, as seen in Fig. 1, causing a number of parallel string segments to lie parallel adjacent the end segment. As discussed in the text, we model knots as forming due to a random series of braid moves of the end segment among the adjacent segments (diagrams at bottom). The overall connectivity of the segments is indicated by the dashed line.

account for the occurrence of a threshold length for forming knots. A mathematical theorem proved by Milnor (28) states that the minimum curvature required to form a knot is 4π versus 2π for an unknotted closed loop. Similarly, to form a knot in our model, the string must have more than one coil, so that at least one segment lies adjacent to the string end. If we assume coils with a diameter equal to the width of the box (d), the circumference is πd, or $\approx$0.5 m for the 0.15-m box, which is similar to the observed threshold length for forming knots (Fig. 2). For the 0.1-m box, the threshold also decreased to $\approx$0.4 m. At the opposite extreme, the longest strings correspond to having $\approx$10–20 adjacent segments in our model.

We wrote a computer simulation that generated knots according to our model and determined their identities by calculating the Jones polynomials for the braid diagrams.[§] The model has only two adjustable parameters: the number of parallel segments (N_S) and the number of braid moves (N_M). Based on the considerations discussed above, we varied N_S from 2 to 20. N_M corresponds to "time" in our model, because we expect the number of braid moves to scale with agitation time in the experiment. The simulations show that the model can qualitatively account for several additional experimentally observed features.

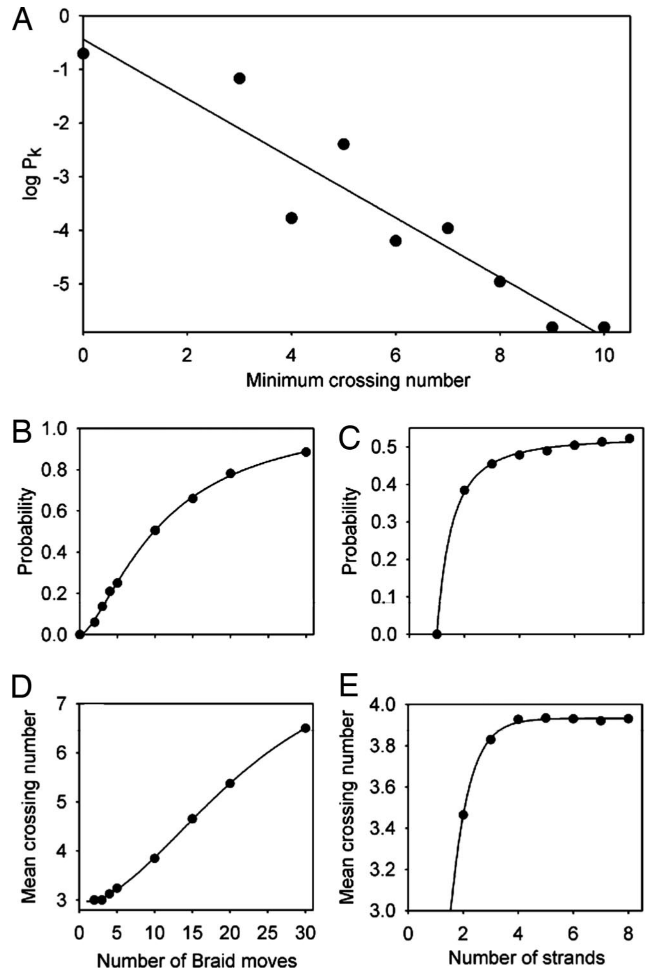

Fig. 7. Predictions of the random braid move model discussed in the text. An ensemble of 1,000 conformations were generated for each condition and analyzed. (*A*) Distribution of minimum crossing numbers of knots generated with $N_S = 10$ and $N_M = 10$, where P_K is the probability of forming a knot with minimum crossing number $c(K)$. (*B*) Probability of knotting P vs. number of random braid moves (N_M) (proportional to agitation time) for $N_S = 10$ segments (proportional to length). (*C*) P vs. N_S for $N_M = 10$. (*D*) Average minimum crossing number $\langle c(K)\rangle$ vs. N_M for $N_S = 10$ segments. (*E*) $\langle c(K)\rangle$ vs. N_S for $N_M = 10$.

First, it predicts a broad distribution of knot types and complexities, as observed experimentally. For example, for $N_S = 10$ and $N_M = 10$, the distribution (Fig. 7*A*) is similar to that observed experimentally with the long strings—knots ranging from crossing number 3 to 10 were observed with overall decreasing probability. The agreement was not perfect because, for example, the 4_1 knot had notably lower probability in the model, whereas 5_1 had notably lower probability in the experiment, but a similarly wide distribution of complexities were observed in both cases. Second, the model predicts that the overall probability of knotting P increases with time (i.e., with N_M) and with string length (N_S) (Fig. 7 *B* and *C*), as observed in the experiment. Finally, it predicts that the average complexity of knots (average minimum crossing number) increases with time and string length (Fig. 7 *D* and *E*), as observed.

Materials and Methods

A computer-controlled microstepper motor spun the boxes, which were made of smooth acrylic plastic and purchased from Jule-Art. The boxes were cubic, of widths 0.1, 0.15, and 0.3 m. The string used in most experiments was solid #4 braided string (catalog no. 021008010030; Samson, Ferndale, WA), which had

[§]These calculations were done by using computer code in Bar-Natan, D., Morrison, S., *et al.*, *The Mathematica Package KnotTheory* (University of Toronto; http://katlas.math.toronto.edu). Accessed July 2007.

a diameter of 3.2 mm, a density of 0.04 g/cm, and a flexural rigidity of 3.1×10^4 dynes·cm^2. In some experiments, a more flexible string was also used (nylon #18 twine) (catalog no. NST1814P; Lehigh Group, Macungie, PA), which had a diameter of 1.7 mm, a density of 0.0086 g/cm, and a flexural rigidity of 660 dynes·cm^2. A stiffer rubber tubing was also used (catalog no. 141782AA; Fisher Scientific, Waltham, MA), which had a diameter of 8 mm, a density of 0.43 g/cm, and a flexural rigidity of 3.9×10^5 dynes·cm^2. The flexural rigidity was determined by cantilevering one end of the string off the edge of a table, such that the end deflected downward a small amount Δy due to the string bending under its own weight. According to the Euler small displacement formula: $\Delta y = mgL^3/(8EI)$, where L is the length, mg is the weight, and EI is the flexural rigidity (29). In principle, tumbling in the plastic box may induce static electric charge in our string, which could influence the dynamics. However, no perturbation of a hanging string was observed when a second segment was brought into close proximity after tumbling, indicating that electrostatic repulsion effects are negligible compared with gravitational weights in our system.

We thank Parmis Bahrami and Joyce Luke for assistance with data collection.

1. Thomson W, Tait PG (1867) *Treatise on Natural Philosophy* (Oxford Univ Press, Oxford).
2. Simon J (2002) in *Physical Knots: Knotting, Linking, and Folding Geometric Objects in R^3* (American Mathematical Society, Providence, RI).
3. Adams CC (2004) *The Knot Book: An Elementary Introduction to the Mathematical Theory of Knots* (American Mathematical Society, Providence, RI).
4. Dean FB, Stasiak A, Koller T, Cozzarelli NR (1985) *J Biol Chem* 260:4975–4983.
5. Shaw SY, Wang JC (1993) *Science* 260:533–536.
6. Arsuaga J, Vázquez M, Trigueros S, Sumners D, Roca J (2002) *Proc Natl Acad Sci USA* 99:5373–5377.
7. Belmonte A, Shelley MJ, Eldakar ST, Wiggins CH (2001) *Phys Rev Lett* 87:114301.
8. Ben-Naim E, Daya ZA, Vorobieff P, Ecke RE (2001) *Phys Rev Lett* 86:1414–1417.
9. Hickford J, Jones R, duPont S, Eggers J (2006) *Phys Rev E* 74:052101.
10. Frisch HL, Wasserman E (1961) *J Am Chem Soc* 83:3789–3795.
11. Delbruck M (1962) *Proc Symp Appl Math* 14:55.
12. Frank-Kamenetskii MD, Lukashin AV, Vologodskii AV (1975) *Nature* 258:398–402.
13. Michels JPJ, Wiegel FW (1982) *Phys Lett A* 90:381–384.
14. Koniaris K, Muthukumar M (1991) *J Chem Phys* 95:2873–2881.
15. Sumners DW, Whittington SG (1988) *J Phys A Math Gen* 21:1689–1694.
16. Shimamura MK, Deguchi T (2002) *Phys Rev E* 66:040801.
17. Alexander JW (1928) *Trans Am Math Soc* 30:275–306.
18. Jones VFR (1985) *Bull Am Math Soc* 12:103–112.
19. Kauffman LH (1987) *Topology* 26:395–407.
20. Micheletti C, Marenduzzo D, Orlandini E, Sumners DW (2006) *J Chem Phys* 124:064903.
21. Goriely A (2005) in *Physical and Numerical Models in Knot Theory*, Series on Knots and Everything, eds Calvo JA, Millett KC, Rawdon EJ, Stasiak A (World Scientific, Singapore), Vol 36, pp 109–126.
22. Fukuhara S (1988) *A Fête of Topology: Papers Dedicated to Itiro Tamura*, eds Matsumoto Y, Mizutani T, Morita S (Academic, New York), pp 443–452.
23. O'Hara J (2003) *Energy of Knots and Conformal Geometry*, Series on Knots and Everything (World Scientific, Singapore), Vol 33.
24. Freedman MH, He ZX, Wang ZH (1994) *Ann Math* 139:1–50.
25. Kusner RB, Sullivan JM (1998) in *Ideal Knots*, eds Stasiak A, Katritch V, Kauffman LH (World Scientific, Singapore), p 315.
26. Belmonte A (2005) in *Physical and Numerical Models in Knot Theory*, Series on Knots and Everything, eds Calvo JA, Millett KC, Rawdon EJ, Stasiak A (World Scientific, Singapore), Vol 36, pp 65–74.
27. Alexander JW (1923) *Proc Natl Acad Sci USA* 9:93–95.
28. Milnor JW (1950) *Ann Math* 52:248–257.
29. Moore JH, Davis CC, Coplan MA (2002) *Building Scientific Apparatus* (Perseus, Cambridge, MA).